



**HAL**  
open science

## Evaluation of acetophenone as a novel alcohol-cycloalkane bifunctional liquid organic hydrogen carrier (LOHC)

Florian d'Ambra, Julia Levy, Parviz Hajiyev, Thibault Cantat, Gérard Gébel, Vincent Faucheux, Emmanuel Nicolas

### ► To cite this version:

Florian d'Ambra, Julia Levy, Parviz Hajiyev, Thibault Cantat, Gérard Gébel, et al.. Evaluation of acetophenone as a novel alcohol-cycloalkane bifunctional liquid organic hydrogen carrier (LOHC). International Journal of Hydrogen Energy, 2023, 48 (85), pp.33207-33222. 10.1016/j.ijhydene.2023.05.024 . cea-04440528

HAL Id: cea-04440528

<https://cea.hal.science/cea-04440528v1>

Submitted on 6 Feb 2024

**HAL** is a multi-disciplinary open access archive for the deposit and dissemination of scientific research documents, whether they are published or not. The documents may come from teaching and research institutions in France or abroad, or from public or private research centers.

L'archive ouverte pluridisciplinaire **HAL**, est destinée au dépôt et à la diffusion de documents scientifiques de niveau recherche, publiés ou non, émanant des établissements d'enseignement et de recherche français ou étrangers, des laboratoires publics ou privés.



Distributed under a Creative Commons Attribution - NonCommercial - NoDerivatives 4.0 International License

# ***Evaluation of Acetophenone as a novel alcohol-cycloalkane bifunctional liquid organic hydrogen carrier (LOHC)***

**Authors:**

**Florian D'Ambra** Univ. Grenoble Alpes, F-38000 Grenoble; CEA, LITEN, LVME, F-38054 Grenoble France, E-mail: [florian.dambra@cea.fr](mailto:florian.dambra@cea.fr)

**Julia Levy** Univ. Grenoble Alpes, F-38000 Grenoble; CEA, LITEN, LVME, F-38054 Grenoble France

**Parviz Hajiyev** Univ. Grenoble Alpes, F-38000 Grenoble; CEA, LITEN, LVME, F-38054 Grenoble France

**Thibault Cantat** Université Paris-Saclay, CEA, CNRS, NIMBE, 91191 Gif-sur-Yvette, France

**Gérard Gébel** Univ. Grenoble Alpes, F-38000 Grenoble; CEA, LITEN, LVME, F-38054 Grenoble France

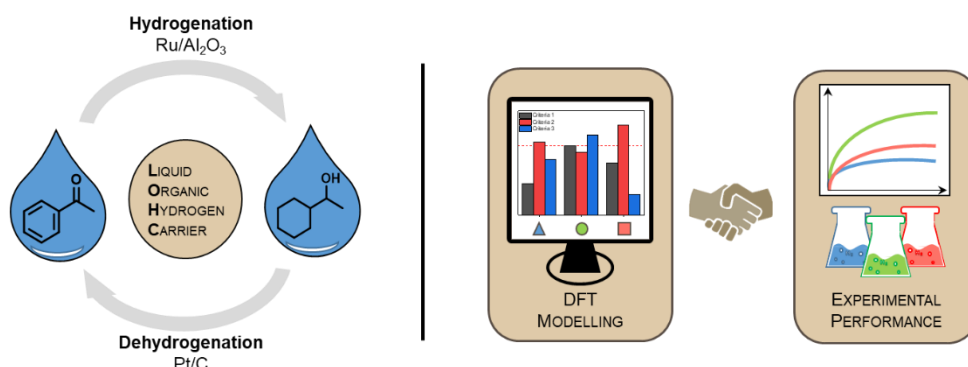
**Vincent Faucheux** Univ. Grenoble Alpes, F-38000 Grenoble; CEA, LITEN, LVME, F-38054 Grenoble France

**Emmanuel Nicolas** Université Paris-Saclay, CEA, CNRS, NIMBE, 91191 Gif-sur-Yvette, France. E-mail: [emmanuel.nicolas@cea.fr](mailto:emmanuel.nicolas@cea.fr)

## **Abstract**

In this contribution, we propose the couple 1-Cyclohexylethanol/Acetophenone as a new biobased and bifunctional LOHC. This material shows promises for hydrogen storage by DFT modelling, while commercial catalysts were identified to carry out both hydrogenation and dehydrogenation: Ru/Al<sub>2</sub>O<sub>3</sub> was found to catalyse the complete hydrogenation of the LOHC at 115 °C in 2 h with 98% selectivity and, for the first time, Pt/C carries out the dehydrogenation at 205 °C in 36 h with total conversion but with a limited Degree of Dehydrogenation of 72%. The system was cycled three times during which up to 50% of the total hydrogen capacity was exploited, stable after 3 cycles. Kinetics experiments and DFT modelling of the reactions intermediates show that a system pairing C–O and C–C bonds is prone to degradation, due to side-reactions initiated by the O-moiety and the reversible hydrogenation of the C=O bond during the dehydrogenation step.

## **Graphical abstract**



## Highlights

1-Cyclohexylethanol/Acetophenone was proposed as a new biobased bifunctional LOHC  
Full hydrogenation and dehydrogenation were achieved with heterogeneous catalysts  
Energies of activation of each function was measured during the dehydrogenation  
Up to 53% of the total hydrogen capacity was exploited during the cycling  
DFT modelling rationalized the dehydrogenation pathway and degradation products

## Keywords

LOHC  
Hydrogen storage  
Heterogeneous catalysis  
Kinetics  
DFT modelling

## Acronyms table

TERM	ACRONYM
1-Cyclohexylethanol	CHEA
1-Phenylethanol	PEO
Acetophenone	APO
Acetylcyclohexane	ACH
Acetylcyclohex-1-ene	ACHN
Ethylbenzene	EB
Ethylcyclohexane	EC
Bis(1-cyclohexylethyl) ether	12H-ROR
Bis(1-phenylethyl) ether	0H-ROR
1,3-Dicyclohexylbutanone	12H-Coupling
1-Cyclohexyl-3-phenylbutanone and 1-Phenyl-3-cyclohexylbutanone	6H-Coupling
1,3-Diphenylbutanone	0H-Coupling
Degree of hydrogenation	DoH
Degree of dehydrogenation	DoDH

## Introduction

The massive storage of energy is a great challenge to tackle in order to favour the implementation of renewable and intermittent energies in our energetic systems. As new energy vectors such as H<sub>2</sub> are expected to take over fossil fuels, appropriate means of storage need to be developed.[1–3] Of all H<sub>2</sub> storage technologies, the Liquid Organic Hydrogen Carrier (LOHC) technology is gaining momentum as an alternative for global transport.[4] The storage concept revolves around catalytic hydrogenation and dehydrogenation reactions using a liquid organic molecule which can respectively store (hydrogenation) and unload (dehydrogenation) H<sub>2</sub> molecules.[5] The chemical storage of H<sub>2</sub> equivalents onto an organic framework reduces the risks associated with the handling and utilization of H<sub>2</sub> gas and can increase at the same time the volumetric energy density of the energy vector. As a result, heavy gas tanks and other devices aiming at storing H<sub>2</sub> in its pure form can be circumvented while retaining high gravimetric and volumetric energy densities.[6] Current LOHC systems regroup the molecules Toluene, Dibenzyltoluene, N-Ethylcarbazole and their hydrogenated counterparts. Many other structures and their associated catalysts have been tested over the years in order to surpass the performances of these systems.[7,8]

As a technology, the enthalpy of dehydrogenation per molecule of H<sub>2</sub> is often regarded as a make-or-break criterion to assess the energy efficiency of a LOHC system. The secondary criteria are the gravimetric and volumetric energy densities that describe the efficiency of the energy storage. Finally, a third criteria is the stability of the system over cycling, with a target of 99.9% of stability per cycle, which corresponds to almost perfect cycling.[9] Early LOHC prototypes were mainly focused on cycloalkanes/aromatics couples to limit the endothermicity of the dehydrogenation step by harnessing the energy gain of the aromatization.[10] Two bottlenecks limit the applications of such LOHC systems: they possess a problematic toxicity and state-of-the art LOHC catalysts are built with platinum group metals (PGM), whose price is detrimental to the development of the technology.

Targets for the LOHC system may vary depending on the application. The current target of the US Department of Energy (DOE) for the enthalpy of dehydrogenation is 30-44 kJ/molH<sub>2</sub> in order to reach an equilibrium pressure of 1 bar of hydrogen in the temperature range -40 °C to 60 °C (useful for on-board hydrogen storage).[11] The ultimate gravimetric and volumetric targets are 6.5 wt.%H<sub>2</sub> and 50 gH<sub>2</sub>/L for a complete on-board system. Stationary systems would have more relaxed criteria as the volume of the system would be less of an issue.

New LOHC systems were proposed to meet these targets. Seminal work by Pez *et al.* opened new perspectives with N- and O-heterocyclic LOHC.[12] DFT modelling by Clot *et al.* rationalised these alternatives by linking the integration of N atoms to the diminution of the enthalpy of dehydrogenation.[13] Further modelling showed that including electrodonating substituents stabilized the aromatic cycle, decreasing the enthalpy as a function of the Hammett parameter  $\sigma$  (para).[14]

Recent contributions in the homogeneous and heterogeneous acceptorless dehydrogenation and hydrogenation of C–O and C–N based chemical functions, such as alcohols, ketones, esters, carbonates, amides and nitriles, are paving the way to the development of unconventional LOHC couples.[15–17] Integrating chemical functions to the LOHC technology opens a way to new combinations of structures, and their addition have been proven beneficial as heteroatoms can weaken the adjacent C–H bonds by inductive electron withdrawing effect and/or donating mesomeric effect.[18] Especially, O-containing LOHC are also of interest as they are usually less toxic than their carbon or nitrogen counterparts and could be sourced on renewable feedstocks.[19] In addition, from the perspective of the catalyst, noble metal-free catalysts such as copper are efficient for the hydrogenation and dehydrogenation of

heteroatomic functions such as alcohol/ketone and alcohol/ester, lowering the amount of critical noble metal in the system.[20–23] Nevertheless, addition of heteroatoms has its share of downsides, and O-containing molecules (alcohols, aldehydes, ketones) can undergo a number of side reactions such as dehydration,[24] oxidation in air, and condensation reactions, leading to intermolecular esterification and to oligomerization,[25,26] or aldolisation-crotonisation reactions.[27] As a result, reaction conditions and catalytic systems must be adequately controlled in order to avoid such side reactions when hydrogenation/dehydrogenation cycles are carried out with LOHC couples involving alcohols and their derivatives.

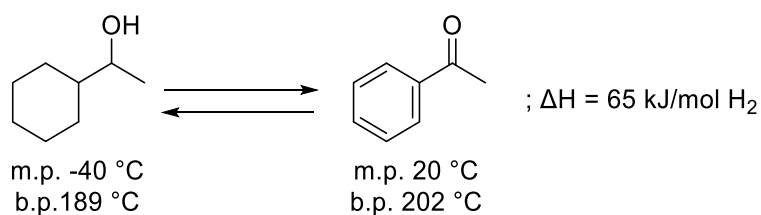
In addition, very few contributions in the literature combine different chemical functions in a LOHC as most work specializes on optimizing/testing a single function while leaving the rest of the LOHC undisturbed.[28] While these works are fundamental to understand the reactivity of each individual function, they do not tackle an integrated system, often at the price of a reduced H<sub>2</sub> capacity. This approach is understandable as finding a catalyst that is efficient for multiple functions is challenging and could destabilize the system. Usually, O-containing LOHCs are either simple alcohols such as methanol or ethanol, diols or O-heterocycles such as dibenzofuran.[29,30]

Various molecules have been suggested as bifunctional LOHCs like the couple Tetrahydro-2-furanmethanol/Furfural, whose promises have been showcased by DFT studies.[31] To the best of our knowledge, while complete hydrogenation was achieved, no article has reported so far the dehydrogenation of tetrahydro-2-furanmethanol to furfural.[32]

To date, the most similar LOHC system containing both an aromatic ring and a free O-function is the couple Cyclohexanol/Phenol. Heterogeneous hydrogenation[33] and dehydrogenation[34] were achieved in the literature. On a system level, this LOHC couple is already produced in industrial quantities which would facilitate its usage. In addition, phenol units are key building blocks in lignin and its formation from biomass molecules is actively researched.[35] However, Phenol is rather sensitive to water and its high toxicity and low explosion limit in air would be a problem for the technical implementation of a Phenol-based LOHC couple.[36] Concomitantly to our work, a recently submitted paper by the Wassercheid group studied the couple Dicyclohexylmethanol/Benzophenone, highlighting the interest of bifunctional LOHC systems.[37]

In this work, we propose to assess the efficiency of a new bifunctional LOHC couple, 1-Cyclohexylethanol/Acetophenone (CHEA/APO). This couple is of interest as its enthalpy of dehydrogenation and H<sub>2</sub> storage capacity (65 kJ/molH<sub>2</sub>, 6.3 wt.%H<sub>2</sub>) are on-par with purely aromatic state-of-the-art systems such as Dibenzyltoluene (71 kJ/molH<sub>2</sub>, 6.2 wt.% H<sub>2</sub>).[38] In addition, both molecules are commercially available and present limited chemical danger. Moreover, Acetophenone is a key molecule found in the transformation of renewable feedstocks such as lignin, removing the dependency of this potential LOHC from fossil fuels in the future.[39]

This couple has already been partially studied, especially the hydrogenation and dehydrogenation of its alcohol/ketone function (Figure 1). A handful of reports have described the homogeneous and heterogeneous hydrogenation of APO to CHEA. While homogeneous and heterogeneous hydrogenation in dilute conditions yielded up to 100% of conversion, solvent-free heterogeneous hydrogenation was only completed in yields inferior to 10%.[40]



Considered reaction	Catalytic metal
<p>1-Cyclohexylethanol (CHEA) ⇌ Acetylcyclohexane (ACH)</p>	Ru[41]
<p>Phényléthanol (PEO) ⇌ Acétophénone (APO)</p>	Cu[20], Cu-Fe[42], Pd[43], Ru[41], Ni [44], Ag[45], Au[46], Ir[47]
<p>Acétophénone (APO) → 1-Cyclohexylethanol (CHEA)</p>	Hydrogenation only: Rh[48], Ru[49], Pt[40], Pd[40], Ni[50]
<p>1-Cyclohexylethanol (CHEA) ⇌ Acétophénone (APO)</p>	This work: Hydrogenation: Ru Dehydrogenation: Pt

Figure 1 – (top) Physical data for CHEA and APO. The melting point of 1-Cyclohexylethanol was obtained by the Joback method.[51]. (bottom) Literature review of the hydrogenation and dehydrogenation of the couple CHEA/APO

To the best of our knowledge, no work has been performed on the complete acceptorless dehydrogenation of 1-Cyclohexylethanol to Acetophenone. Our aim is to determine a set of catalytic conditions that enable the full dehydrogenation and full hydrogenation, as well as evaluating the capacities of such a system to behave as a LOHC, performing several hydrogenation/dehydrogenation cycles under solvent-free conditions.

## Results and discussion

Over the reactions of hydrogenation and dehydrogenation, numerous compounds have been observed by GC-MS. They are displayed with the acronyms that are used further in the text, in Figure 2, and sorted in 5 different classes according to their role in the reaction of interest.



First of all, all catalysts achieve similar APO conversion levels in 4 h (> 98 %). However, the Pd catalysts produce mainly 1-Phenylethanol (PEO), showing their poor activity for the hydrogenation of the aromatic cycle as a standalone metal.[52] An observed strong tendency for dehydration is also linked to the surface acidity for Pd heterogeneous catalysts.[53] Conversely, Pt and especially Ru exhibit high conversions and selectivities, as expected from the literature.[54,55] General reactivity follows the order Ru > Pt > Pd, in agreement with the literature.[56] The support, Alumina or carbon, displays in general little to no influence on the conversion, however the LOHC stability is generally improved when alumina is used. Finally, only the Ru based catalysts showed DoH superior to 90%. After this first screening, we thus selected Ru/Al<sub>2</sub>O<sub>3</sub> as the best catalytic system as it had the highest selectivity and a DoH equivalent to Ru/C. We then tried to improve it further by modifying the reaction temperature. Ru/C and Pt/Al<sub>2</sub>O<sub>3</sub> were used as comparison due to the former presenting the highest DoH and the latter the highest LOHC stability in our preliminary study.

While a modification of the temperature has almost no effect for the conversion of APO depending on the catalyst (ESI S7), a strong influence on the hydrogenation selectivity to CHEA was observed. In particular, higher reaction temperatures promote dehydration on the Ru catalysts, probably due to the presence of acidic sites on the support. Conversely, the DoH rapidly reaches >99% values from 105 °C for Ru/C and from 115 °C for Ru/Al<sub>2</sub>O<sub>3</sub>. At 115 °C, Ru/Al<sub>2</sub>O<sub>3</sub> achieves the maximal selectivity and DoH of all studied systems (93% selectivity, >99% DoH) (Figure 3)

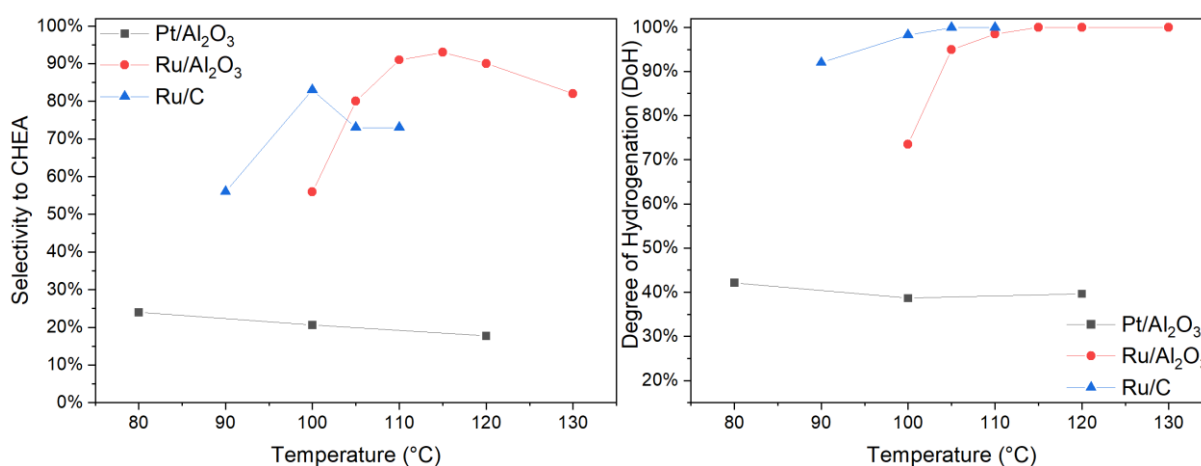


Figure 3 - Left: Selectivity to CHEA for Pt/Al<sub>2</sub>O<sub>3</sub> (black), Ru/Al<sub>2</sub>O<sub>3</sub> (red) and Ru/C (blue); right: DoH for Pt/Al<sub>2</sub>O<sub>3</sub> (black), Ru/Al<sub>2</sub>O<sub>3</sub> (red) and Ru/C (blue)

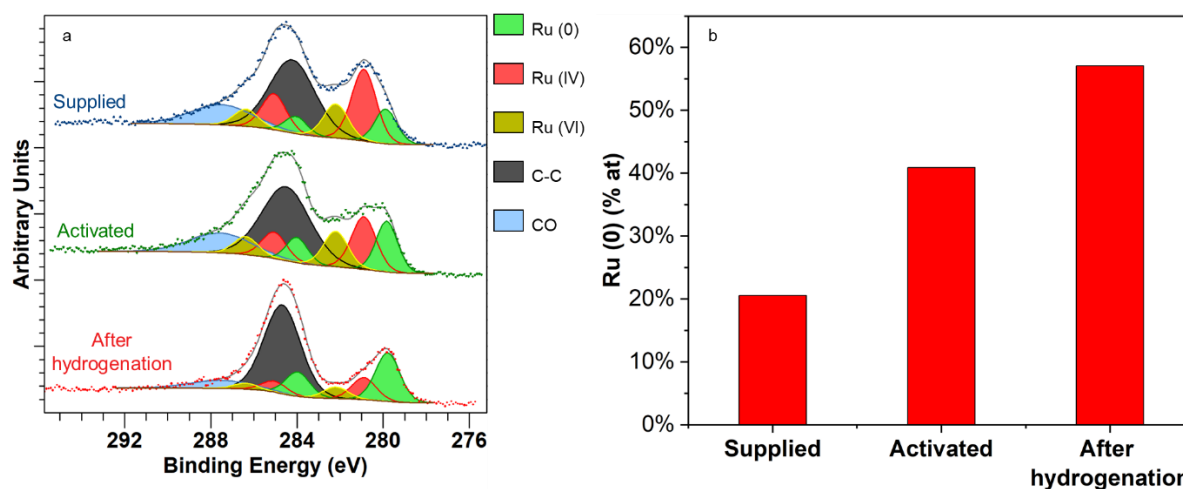
The calcination and subsequent activation of Ru/Al<sub>2</sub>O<sub>3</sub> under hydrogen increases the selectivity and reduces the reaction time (ESI S8). After optimization, we thus selected the activated Ru/Al<sub>2</sub>O<sub>3</sub> as a hydrogenation catalyst (0.1 wt% active metal to Acetophenone), used at 115 °C for 2 h, under 50 bar of H<sub>2</sub>.

## 2. Analysis of the selected Ru/Al<sub>2</sub>O<sub>3</sub> catalyst for the hydrogenation of Acetophenone

The Ru/Al<sub>2</sub>O<sub>3</sub> catalyst was analyzed by XPS at three different steps: as supplied, after activation and after hydrogenation. The Ru 3d and Ru 3p core levels were recorded (Figure 4a and ESI S9) so as to estimate the oxidation state of the catalyst. For data treatment, a Shirley background was applied for both spectra and fitting of the Ru 3d core level spectra was achieved by using three pairs of pseudo-voigt function, a linear combination of a Gaussian and



Lorentzian. The ratio between the 3d doublet area and the distance between the doublet peaks were fixed at 2 and 4.2 respectively.



Ru/Al <sub>2</sub> O <sub>3</sub> catalyst state	Ru average size and dispersion (nm)	Specific surface (m <sup>2</sup> /g)	Pore diameter (nm)
Supplied	1.7±0.3	135	19.1
Activated	2.4±1.6	138	19.7
After hydrogenation	2.4±2.1	137	20.2

Figure 4 - (a) Ru 3d spectra of the ruthenium of the supplied catalyst, the activated catalyst and the catalyst after hydrogenation. b) Atomic percentage of reduced Ru(0) for the supplied catalyst, the activated catalyst and the catalyst after hydrogenation. (bottom) Size and dispersion of the Ru nanoparticles and specific surface and pore diameter of the Al<sub>2</sub>O<sub>3</sub> support.

In the Figure 4a, the Ru3d<sub>5/2</sub> peaks at 279.9, 280.9 and 282.2 eV correspond to Ru (0), Ru (IV) and Ru (VI) oxidation states respectively (the peaks are assigned in green, red and yellow in the Figure 4a respectively). [57] The RuO<sub>3</sub> species was described as a defect structure on the surface of RuO<sub>2</sub>. [58] As the C 1s core level is superimposed on the Ru 3d core level, a peak corresponding to organic surface contamination is added (C-C peak). The spectra also shows the presence of oxidized carbon species (CO peak) that disappear after the catalyst is activated. All of the Ru peaks binding energies in the 279 to 283 eV range are reported in the ESI S10. Ru (IV) and Ru (VI) were grouped as “oxidized Ru” and the percentage of reduced Ru (0) was compared to the former (Figure 4b). An increase of almost 20% of the reduced Ru (0) is obtained after the activation of the catalyst and a further increase of 20% is observed after the hydrogenation, leaving only 40% of oxidized Ru species that are ascribed to surface oxidation in air and covalent bonds between the Ru nanoparticles and the alumina substrate. [59]

These results are in agreement with the removal of surface contaminants as well as reduction of oxidized Ru and modification of the support that were observed by FTIR-ATR, Raman spectroscopy, XRD and ICP-OES (ESI S12, S13, S14 and S15). Its mechanism (removal of surface water and hydroxyl groups during the calcination, reduction of the oxidized Ru to Ru(0) during the activation under H<sub>2</sub>) was studied by TGA and TGA-MS (ESI S16, S17 and S18). A limited agglomeration of the Ru nanoparticles was observed by TEM-EDX but should have no measurable incidence on catalytic activity at these high conversions (Figure 4 and ESI S19). Indeed, activity variation is usually observable only for sizes exceeding 5-10 nm. [60] However, the Ru reduction state matters as Ru(0) species have also been shown to increase the activity

for hydrogenation reactions comparatively to Ru (IV) species.[61] Finally, the support structure (specific surface and pore diameter) is not modified by the activation process and reaction as showed by BET adsorption (Figure 4 and ESI 20).

The XPS Al 2p core level spectra (ESI S10) shows no notable differences after activation and after hydrogenation. The position of the peaks around 74.5 eV corresponds to the Al<sup>3+</sup> oxidation state and not to a metallic Al which is reported around 72.5 eV.[62,63] The presence of Al<sub>2</sub>O<sub>3</sub> or Al(OH)<sub>3</sub> can not be determined by XPS analysis but XRD analysis (ESI S14) shows Al(OH)<sub>3</sub> turning into Al<sub>2</sub>O<sub>3</sub> during the activation of the catalyst.

### 3. Catalytic evaluation of supported metal catalysts for the dehydrogenation of 1-Cyclohexylethanol

The dehydrogenation is endothermal, and is often the barrier to get an efficient LOHC system.[7] Here we tested various noble and non-noble metal catalysts for the dehydrogenation of CHEA to produce APO (Figure 5 and ESI S21).

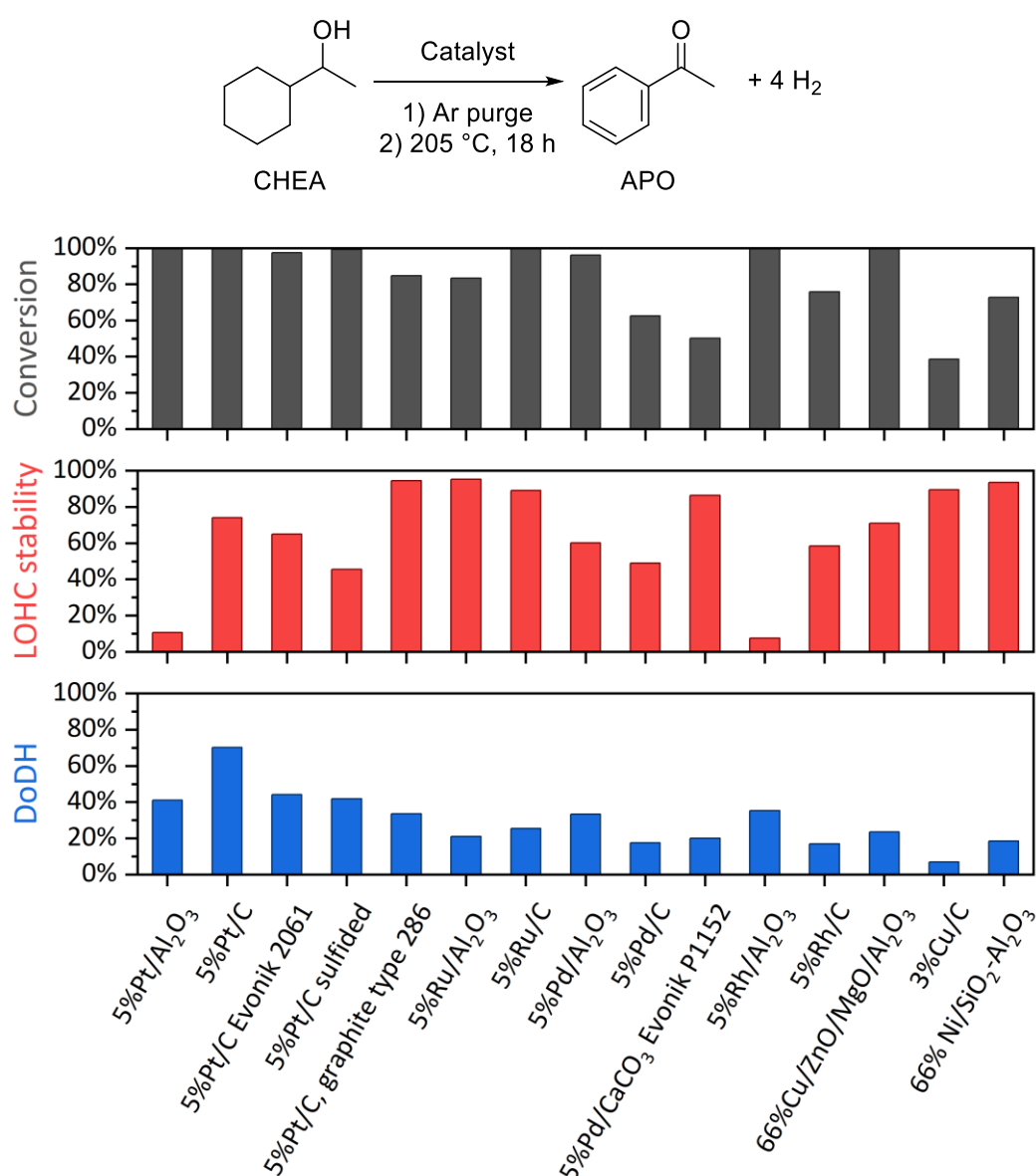
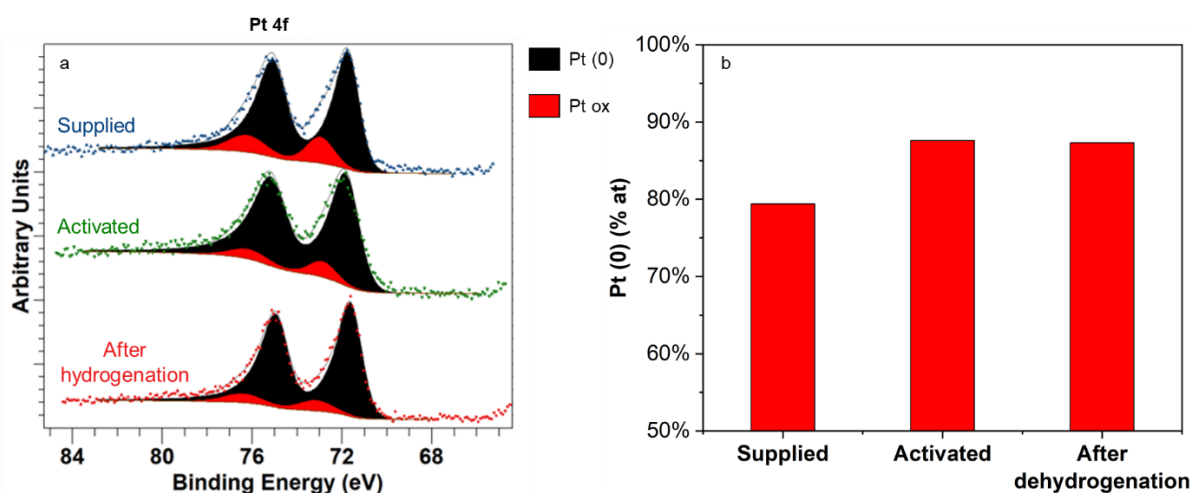


Figure 5 – CHEA conversion, LOHC stability and Degree of dehydrogenation (DoDH) of the catalysts tested for the dehydrogenation of CHEA to APO. 1.5 mL CHEA, 1 wt.% active metal catalyst (with regard to APO), 18 h, 205 °C.

The Ru, Cu and Ni catalysts showed good conversion and selectivity for the dehydrogenation of the alcohol to the ketone but a limited reactivity for the aromatization, in agreement with the literature.[64–66] The Pd catalysts achieved the dehydrogenation of both the cycle and the alcohol but also exhibited a strong tendency for dehydration products (Figure 2).[67,68] Similarly to Pd, the Rh catalysts managed both dehydrogenation steps but favoured the formation of the coupling products instead.[68] Pt catalysts displayed the best conversion of all catalysts, but intramolecular dehydration products could always be found. Various side-reactions were favoured depending on the support but no correlation with the support was found. Out of all the tested catalysts, the 5%Pt/C catalyst supplied by Sigma-Aldrich yielded the best compromise between conversion, LOHC stability and degree of dehydrogenation. Further experiments on the catalytic loading and time of reaction after activation were used to refine the conditions to yield the most efficient dehydrogenation parameters. The complete CHEA conversion, a DoDH of 72% and a LOHC stability of 80% was achieved with a catalyst loading of 0.25 wt.%Pt and a reaction time of 36 h. (ESI S22). While this result is promising, CHEA dehydrogenation kinetics (0.005 gH<sub>2</sub>/gPt/min at DoDH = 56%) are still a hundred to a thousand times slower than the benchmark systems Dibenzyltoluene (0.61 gH<sub>2</sub>/gPt/min at DoDH = 51%)[69]and N-Ethylcarbazole (0.17 gH<sub>2</sub>/gPd/min at DoDH = 57%).[70]

#### 4. Analysis of the selected Pt/C catalyst for the dehydrogenation of 1-Cyclohexylethanol

The catalyst was analyzed by XPS after three different steps: as supplied, after activation and after dehydrogenation (Figure 6a). The Pt 4f core level was fitted with an asymmetric doublet corresponding to the reduced state of platinum.[71] Another pair of pseudo-voigt distribution (Gaussian-lorentzian peaks) corresponding to an oxidized Pt state was added.



Pt/C catalyst state	Pt average size and dispersion (nm)	Specific surface (m <sup>2</sup> /g)	Pore diameter (nm)
Supplied	1.7±0.4	1577	3.4
Activated	1.5±0.5	1598	3.4
After hydrogenation	2.0±0.8	1460	3.4

Figure 6 - (a) Pt 4f spectra of the supplied catalyst, the activated catalyst and the catalyst after dehydrogenation. (b) Atomic percentage of Pt(0) for the supplied catalyst, the activated catalyst and the catalyst after dehydrogenation. (bottom) Size and dispersion of the Pt nanoparticles and specific surface and pores diameter of the carbon support.

Roughly 80% of the Pt is reduced in the supplied catalyst (Figure 6b). The activation of the catalyst leads to the increase of the reduced Pt (0) species as O<sub>2</sub>-reactive low coordination sites are removed (Figure 6b).[72] The proportion of the oxidized Pt species is reduced to roughly 12-13% after the activation of the catalyst. No significant variation of reduced Pt (0) is observed between the activated catalyst and the catalyst after dehydrogenation.

Oxidized Pt species are only visible by XPS while FTIR-ATR, Raman spectroscopy, ICP-OES, TGA and BET adsorption show little to no variation between the samples (ESI S23, 24, S25, S26 and S27). A limited sintering of the Pt nanoparticles is visible by TEM-EDX and XRD after dehydrogenation (Figure 6, and ESI S28 and S29). No significant variation of specific surface and pore diameter was detected after reduction and utilization.

## 5. Chemical kinetics of dehydrogenation

To better understand the dehydrogenation pathway, chemical kinetics experiments were performed. Chemical kinetics show a near total conversion of the reactant in less than 24 h (Figure 7). The DoDH rapidly increases to 30% in 10 h. At that time, more than 85% of the alcohol is already converted into the ketone. Over the 10 following hours, the DoH increases only by 10%, pointing to a change in the dehydrogenation step controlling the rates. This observation is consistent with a two-step system kinetics with a fast first step and a slow second step.[73] In addition, the formation of the dehydrogenated condensation product, OH-Coupling, as the main impurity stays below 5% during the reaction.

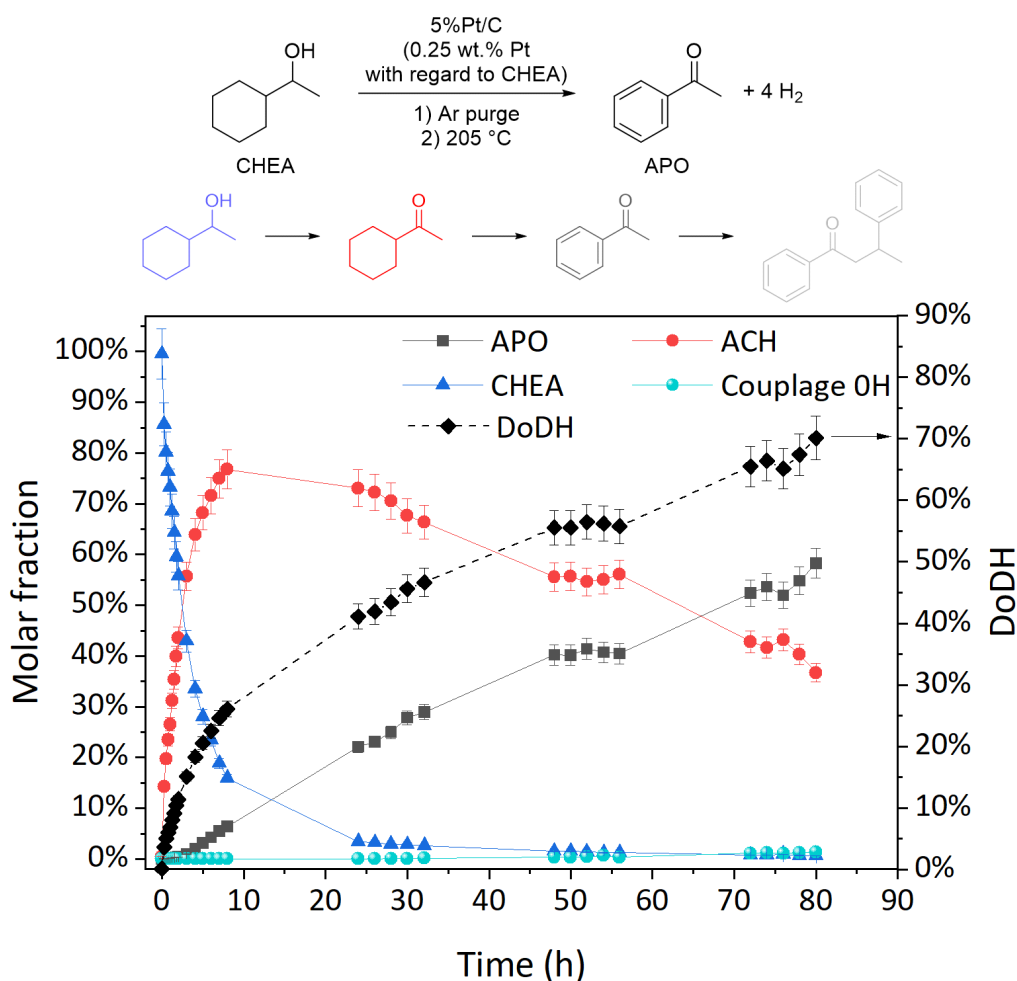


Figure 7 – Scheme of the reaction (top); Products distribution during the dehydrogenation and DoDH (bottom). All other products were found in quantities below 5% during the reaction. 0.25 wt.% Pt with regard to CHEA, 205 °C.

Moreover, other kinetic experiments showed that each step of the dehydrogenation is reversible due to the residual H<sub>2</sub> pressure. Indeed, during the dehydrogenation of 1-Phenylethanol (PEO) intermediate to APO, spontaneous hydrogenation of the aromatic cycle is observed either *via* direct hydrogenation or transfer hydrogenation (ESI Figure 7S30). It is however difficult to conclude on which mechanism directs the reaction as the laws of the kinetics for each step are complex and the C-O bond can easily be hydrogenated or dehydrogenated and hence act as a platform for transfer-dehydrogenation.

Further kinetics experiments were carried out in order to calculate the activation energy of each function. Here, each molecule is characterized by 2 factors: the dehydrogenation state of the alcohol function and the one of the cycle (Figure 8 top left). The 6H-Coupling product contributes for half its molar fraction to both CH and Ar classes (as defined in Figure 8). No dehydration products were observed during the experiment.

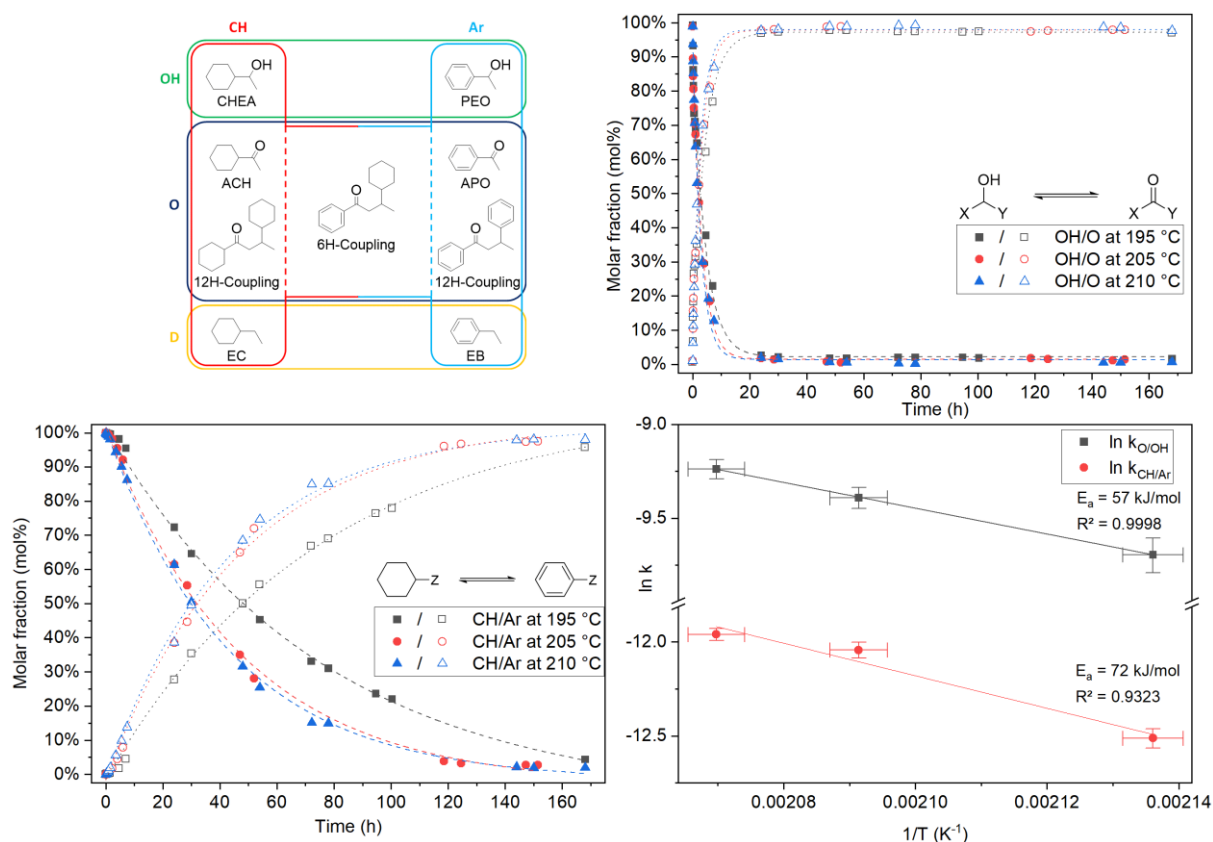


Figure 8 –Classification by functions of the products for the lumped kinetics: CH=Cyclohexane, Ar=Aromatic, OH=Alcohol, O=Ketone, D=Dehydration (top left); Lumped kinetics for the O and OH compounds (top right); Lumped kinetics for the CH and Ar compounds (bottom left); Activation energies for the OH/O and CH/Ar functions (bottom right).

For both the OH/O and CH/Ar functions, the increase of the temperature of reaction increases the kinetics as expected. Moreover, the equilibrium state for the OH/O function is reached after 24 h (Figure 8 top right), whereas the CH/Ar function reaches equilibrium between 140 and 168 h depending on the temperature of reaction (Figure 8 bottom left). The apparent specific rate constants were calculated for each reaction and function by performing an exponential fit on the function curves assuming 1st order kinetics in a batch stirred reactor. All adjusted R<sup>2</sup> are above 0.989 (ESI S31). External diffusion effects are supposedly non limiting due to the high stirring speed (1500 rpm). Indeed, classic LOHC setup have showed external diffusion effects below 500 rpm during the dehydrogenation.[12] Internal diffusion effects are also negligible as shown by internal effectiveness factors being close to 1 for each function (ESI

S32). The activation energy for each function was obtained by using the Arrhenius law (Figure 8 bottom right). As no kinetics study on the dehydrogenation of CHEA to APO was reported in the literature, the comparison of the activation energy was performed by assimilating the OH-O function to the dehydrogenation of isopropanol to acetone and the CH-Ar function to the dehydrogenation of cyclohexane to benzene. The OH-O activation energy was calculated to be 57 kJ/mol compared to 28 kJ/mol in the literature.[74] The difference in activation energy could be due to the steric hindrance of the cycle compared to the methyl group.[75] Conversely, the calculated CH-Ar activation energy is in good agreement with the literature (72 kJ/mol vs 70 kJ/mol), which suggests that the O-group does not strongly influence the dehydrogenation.[76] The lower activation energy for OH-O is consistent with the dehydrogenation of this bond before the dehydrogenation of the cycle.

## 6. Cycling

The system was cycled thrice using the optimized conditions (Figure 9, top left). Material losses of 10 to 20% per step were visible and attributed to reactor transfers, filtrations and sampling for GC-MS analysis (ESI S33). A slight degradation occurred, mainly due to the self-coupling and the dehydration of the LOHC (Figure 9, top right). However, as the degradation products still possess a 6-membered cycle like EB/EC, cycling of the whole mixture is still possible without a dramatic loss of hydrogen storage.[77,78] By pondering the theoretical capacity of each degradation product in the mixture, close to 99% of the maximum theoretical hydrogen capacity (i.e. the theoretical capacity of the CHEA/APO couple) is retained even after the third cycle (Figure 9, bottom left). As new LOHC couples are produced through the degradation of the CHEA/APO, the degree of hydrogenation and dehydrogenation over the cycling needs to be modified to account for the cycling of each subspecies. Indeed, each sub-LOHC couple can store various amounts of hydrogen hence the quantity of the sub-LOHC couples as well as its theoretical maximum storage capacity are taken into account to calculate the equivalent of the DoDH and DoH of the system. The exploited H<sub>2</sub> capacity, which describes the amount of hydrogen unloaded during a cycle by the LOHC system, is calculated by equation (5). During the cycling, up to 50% of the hydrogen capacity could be used (Figure 9, bottom right). Further catalyst design is hence required to access the rest of the H<sub>2</sub> capacity and decrease the reaction time while avoiding the degradation of the LOHC.

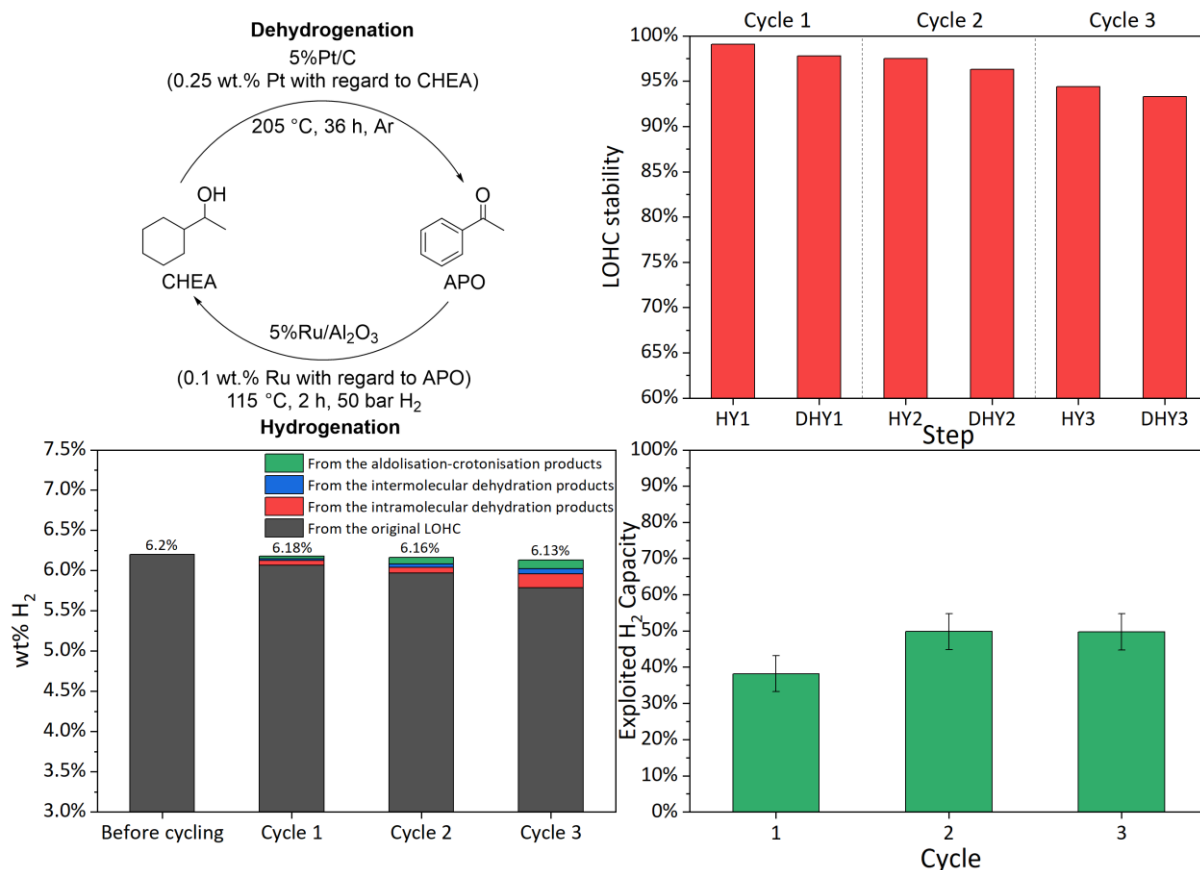


Figure 9 – Optimized conditions of cycling (top left); LOHC stability at the end of each step of the cycling (top right); Maximum H<sub>2</sub> theoretical capacity at the end of each cycle (bottom left); Exploited H<sub>2</sub> capacity over the cycling (bottom right).

## 7. Enthalpy of dehydrogenation and mechanism of reaction

The energies of the key organic intermediates involved in the reaction were computed by DFT. The accuracy of the method was first assessed by calculating the dehydrogenation enthalpy of known LOHC couples (Figure 10); the difference between the experimental values reported in the literature and calculated values fall below 3 kJ/molH<sub>2</sub> which is satisfactory (ESI S34). Based on DFT, the estimated enthalpy change for the CHEA/APO couple is 65 kJ/molH<sub>2</sub>, which is close to that of Cyclohexanol/Phenol (64 kJ/molH<sub>2</sub>).

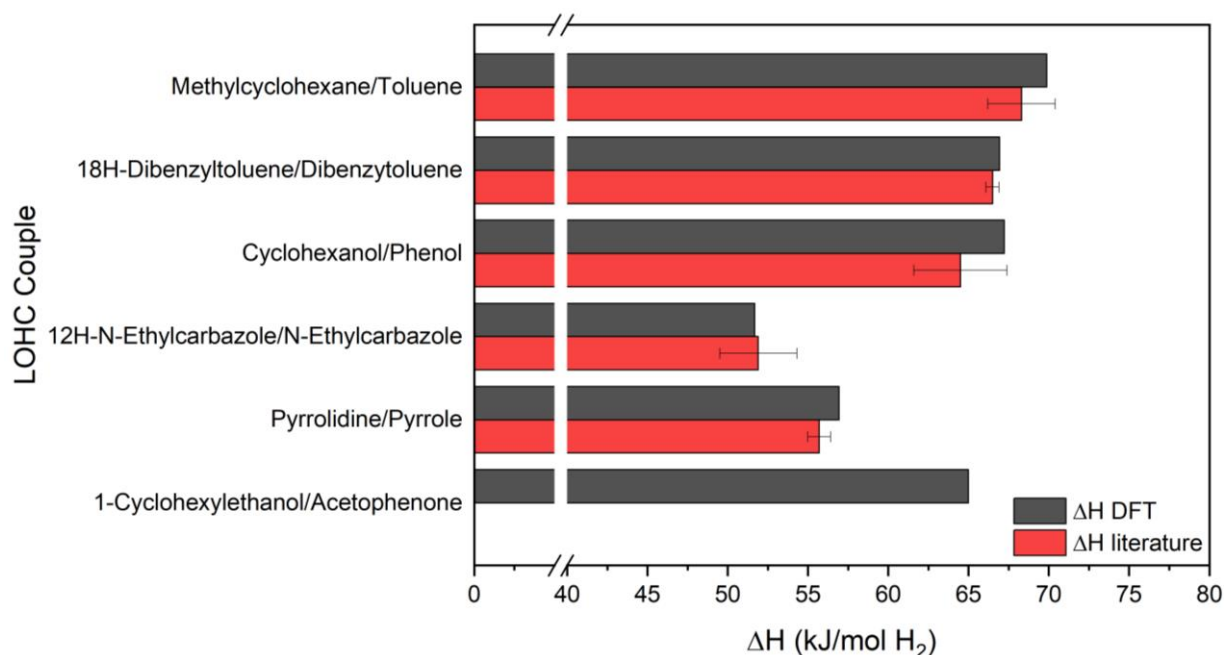


Figure 10 - Comparison of  $\Delta H$  values obtained from the literature or by DFT calculations.

We then computed a number of plausible intermediates, some of which are presented in the Figure 11. The enthalpy change for each potential intermediate is presented in the ESI S35. Among those, some have been identified by GC-MS (highlighted by green rectangles). The other intermediates are not observed, probably due to their lack of stability or high reactivity. VEC and VEB are proposed as intermediates for the intramolecular dehydration of the alcohols, which are hydrogenated to yield EC and EB as the corresponding cycloalkanes.[79] Intermolecular dehydration between two alcohol bearing molecules (CHEA and APO) is most thermodynamically favoured degradation pathway and 12H-ROR ( $\Delta H=-9$  kJ/mol,  $\Delta G=1$  kJ/mol) and 0H-ROR ( $\Delta H=-2$  kJ/mol,  $\Delta G=9$  kJ/mol) should be produced as the main impurities based on the enthalpy change. The probable limitations to the ether formation are the steric hindrance and the lack of strong acidic sites on the catalyst. The coupling products, whilst the less thermodynamically favourable of the impurities ( $\Delta H=25$  kJ/mol,  $\Delta G=34$  kJ/mol) are formed as the main by-products through an aldol addition of two ketones bearing molecules (ACH and APO), followed by an internal dehydration (12H-AI and 0H-AI) and subsequent hydrogenation of the formed  $\alpha,\beta$ -unsaturated ketones to yield 12H-Coupling, 6H-Coupling and 0H-Coupling.[80] The aldol addition is reversible with a strong base,[81] however the high temperature of reaction in combination with the hydrogen in solution favours the crotonisation/hydrogenation pathway. The hydrogenation of the 12H-AI and 0H-AI intermediates is highly favourable in the presence of hydrogen (resp.  $\Delta H=-110/-120$  kJ/mol,  $\Delta G=-74/-84$  kJ/mol), explaining the absence of these structures in the reactional mixture. These conditions render the reaction irreversible as electrons are not stabilized anymore by resonance, which allows for the accumulation of the coupling products in solution. The aldol reaction is also possible in the presence of a metallic enolate. However, as platinum is the only metal in the reaction mixture and has not been shown to favour enol formation, this reaction pathway is less plausible.[82]



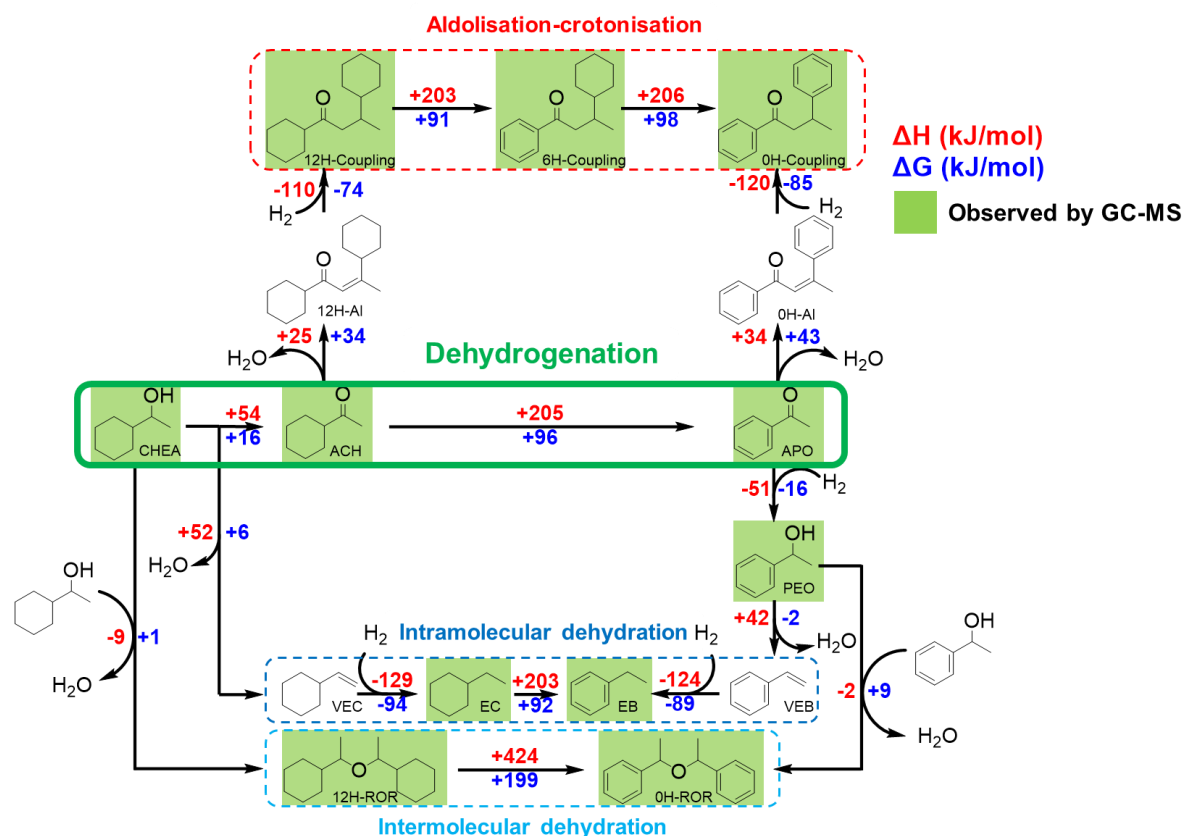


Figure 11 - Enthalpy (red) and free energy change (blue) between the intermediates of the system during the dehydrogenation. The products identified by GC-MS are highlighted in green.

Degradation by removal of the oxygen atom or change in the carbon backbone is supposed irreversible while reactions producing hydrogen are expected to be reversible under the conditions of the system.

As unwanted dehydration and condensation reactions are catalysed by acidic or basic conditions, the effect of the acidity or basicity of the support on the reaction selectivity was investigated. Three alumina with various acidity/basicity were used to synthesize 2 wt.% Pt/Al<sub>2</sub>O<sub>3</sub> catalysts. Dehydrogenation of CHEA was performed for each catalyst but no correlation between the support acidity/basicity and the composition of the impurities was found (ESI S36 and S37). Dehydration of the LOHC could not be prevented by changing the substrate to a basic alumina.

## Conclusion

A new bifunctional LOHC couple, based on 1-Cyclohexylethanol/Acetophenone, has been evaluated by DFT and deemed a potential LOHC couple. Lab experiments showed promises on its application as a LOHC as Ru/Al<sub>2</sub>O<sub>3</sub> hydrogenated the LOHC at 115 °C in 2 h with a conversion of 100% and 98% selectivity. The dehydrogenation was successfully carried out using Pt/C at 205 °C in 36 h with total conversion but with a degree of dehydrogenation (DoDH) limited to 72% and a LOHC stability of 80%. These conditions were used to cycle the system three times during which up to 50% of the total hydrogen capacity could be exploited, stable after 3 cycles. The limitations of such a system, which pairs C–O bonds and C–C bonds, have been identified: the reversibility of the hydrogenation of the ketone group upon dehydrogenation facilitates condensation and dehydration reactions, under the conditions required for the slower dehydrogenation of the cyclohexyl ring. Degradation of the carrier produces LOHC-like structures, some of which have already been studied in the literature such

as Ethylcyclohexane/Ethylbenzene and are hence not incompatible with cycling. Further work is required on the catalysis to refine the activity to the targeted species, increase the kinetics, limit the side reactions or regenerate the LOHC mixture to further its development as a LOHC.

## Experimental

### Materials

1-Cyclohexylethanol (98%) was purchased from Alfa-Aesar. Acetophenone (99%),  $\text{H}_2\text{PtCl}_6$ ,  $6 \text{ H}_2\text{O}$  (37.5% min. Pt basis) and activated acidic, neutral and basic Brockmann I  $\text{Al}_2\text{O}_3$  were purchased from Sigma-Aldrich. Chemicals were used as received without any purification.

5%Pt/ $\text{Al}_2\text{O}_3$ , 5%Pt/C (matrix activated carbon support), 5%Pt/C Evonik Noblyst P2061, 5%Ru/C, 5%Pd/ $\text{Al}_2\text{O}_3$ , 5%Pd/ $\text{CaCO}_3$  Evonik Noblyst P1151, 3%Cu/C, 5%Rh/ $\text{Al}_2\text{O}_3$ , 5%Rh/C and were supplied by Sigma-Aldrich (SA). 66%Cu/ZnO/MgO/ $\text{Al}_2\text{O}_3$ , 5%Ru/ $\text{Al}_2\text{O}_3$ , 5%Pd/C, 5%Pt/C sulfide, 5%Pt/graphite type 286 were supplied by Alfa-Aesar (AA) and 66%Ni/ $\text{Al}_2\text{O}_3$ - $\text{SiO}_2$ . All catalysts were used as received, except when stated otherwise.

### Methods

#### Treatments of the catalyst ruthenium supported on alumina

The catalyst was calcined at 400 °C for 4 h in dry air (5 °C/min, 100 mL/min) and then reduced at 250 °C for 4 h in 2.5%  $\text{H}_2$ /Ar (2 °C/min, 100 mL/min). The reduced catalyst was stored in a storage box flushed with Argon. Further treatments for the preparation of the Ru/ $\text{Al}_2\text{O}_3$  catalyst as supplied, activated and after hydrogenation are shown in the ESI S32.

#### Treatments of the Platinum supported on carbon catalyst

The catalyst was reduced at 280 °C for 4 h in 2.5%  $\text{H}_2$ /Ar (3 °C/min, 100 mL/min). The reduced catalyst was stored in a storage box flushed with Argon. Further treatments for the preparation of the Pt/C catalyst as supplied, activated and after hydrogenation are shown in the ESI S33.

#### Catalyst surface analysis by XPS

The catalysts were analysed by XPS after three different steps: as received, after activation and after reaction (hydrogenation or dehydrogenation). A monochromatic beam (X-ray source Al  $\text{K}\alpha$  1486.6 eV) of 100  $\mu\text{m}$  in diameter and 24.9 W of power was focused on the surface of the samples. High resolution core level analyses were performed using a pass energy of 23.9 eV, which corresponds to an energy resolution of 0.6 eV. All XPS measurements were carried out under ultrahigh vacuum conditions ( $7 \times 10^{-8}$  Pa). Each core level peak was recorded within ten scans with a scan rate of 0.1 eV/s. The binding energy calibration was performed using the C 1s peak shifted at 285 eV. The core level binding energies were recorded within an error of  $\pm 0.1$  eV. Curve fitting and background subtraction were accomplished using Casa XPS software.

#### Hydrogenation

Typically, Acetophenone (12.5 mL) and the heterogeneous catalyst (0.1 wt% active metal to the substrate) were mixed together in a 50 mL Parr hydrogenation batch reactor. The reactor was purged by three cycles of 10 bar  $\text{N}_2$ /atmospheric pressure, then one cycle 50 bar  $\text{H}_2$ /atmospheric pressure. The reactor was then pressurized with 50 bar  $\text{H}_2$  and heated up at reaction temperature under strong stirring (1000 rpm). The flow of the  $\text{H}_2$  inlet was controlled by a mass flow meter. The reaction started when a non-zero flow was detected by the mass

flow. At the end of the reaction, the reaction mixture is filtered on a syringe filter (0.2  $\mu\text{m}$ ) before being analysed by gas chromatography coupled with mass spectrometry (GC-MS).

### Dehydrogenation

In a typical procedure, 2.5 mL of 1-Cyclohexylethanol and 5% Pt/C (1 wt% active metal to the substrate) were mixed together in a 50 mL round-bottom flask connected to a condenser. The setup was purged by three cycles of vacuum/Argon before being heated under reflux of the LOHC (205  $^{\circ}\text{C}$ ) and stirred at 1500 rpm for 18 h. At the end of the reaction, the reaction mixture is filtered on a syringe filter (0.2  $\mu\text{m}$  pore diameter) before being analysed by GC-MS.

### Analysis

Identification and composition of the reaction crude mixtures were performed by a 7820A Agilent GC-MS (5977E MSD) with a 7693A Autosampler. The column was a 30 m, 0.25 mm diameter, 0.5  $\mu\text{m}$  film HP-INNOWAX. Helium was used as the carrier gas (1 mL/min). Acetophenone (APO), Acetylcyclohexane (ACH), Acetylcyclohex-1-ene (ACHN), 1-Cyclohexylethanol (CHEA), 1-Phenylethanol (PEO), Ethylbenzene (EB), Ethylcyclohexane (EC) and 1,3-Diphenylbutanone (OH-Coupling) were calibrated to obtain the response factor of the equipment. Unavailable chemicals (e.g. Bis(phenylethyl) ether) were supposed to have a response factor similar to that of already calibrated akin or related products (e.g. 1-Phenylethanol). To perform the analysis, the crude reaction mixtures were diluted (1:250 wt%/wt%) with an acetonitrile solution containing 0.25%vol. 3-octanone as internal standard. A split ratio of 1:20 was applied to the 1  $\mu\text{L}$  injection. The heat program was: initial oven temperature 50  $^{\circ}\text{C}$ , final oven temperature 260  $^{\circ}\text{C}$  for 6 min, program rate 25  $^{\circ}\text{C}/\text{min}$ . A typical GC-MS spectrum is found in the ESI (ESI S1).

### Definitions

The conversion is calculated using the equation (1):

$$\text{Conversion} = \frac{n_{\text{CHEA after reaction}}}{n_{\text{CHEA before reaction}}} = 1 - \text{mol}\%_{\text{CHEA after reaction}} \quad (1)$$

The LOHC stability represents an evaluation of the LOHC degradation through the formation of unwanted side-products. Similar to a carbon balance calculation, it consists of the sum of the molar percent of the starting material, desired product and key-intermediates as shown in equation (2) **Erreur ! Source du renvoi introuvable.**

$$\text{LOHC stability} = \text{mol}\%_{\text{CHEA}} + \text{mol}\%_{\text{APO}} + \text{mol}\%_{\text{ACH}} + \text{mol}\%_{\text{ACHN}} + \text{mol}\%_{\text{PEO}} \quad (2)$$

The degree of hydrogenation is used during the hydrogenation to quantify the amount of  $\text{H}_2$  stored by the system. Hydrogenation coefficients detailed in the ESI (ESI S2) are used to qualify the amount of hydrogen stored by the system. For the CHEA/APO couple, it is calculated by the equation (3):

$$\text{DoH} = \frac{\text{Quantity of } \text{H}_2 \text{ stored}}{\text{Maximum theoretical } \text{H}_2 \text{ amount}} = \frac{\sum_i (C_{\text{H},i} \times \text{mol}\%_i)}{4} \quad (3)$$

For the dehydrogenation, the catalyst performance is calculated in a similar fashion, by swapping DoH with DoDH and its associated coefficients (ESI S3) in the equation (4) :

$$\text{DoDH} = \frac{\text{Quantity of } \text{H}_2 \text{ released}}{\text{Maximum theoretical } \text{H}_2 \text{ amount}} = \frac{\sum_i (C_{\text{DH},i} \times \text{mol}\%_i)}{4} \quad (4)$$

The H<sub>2</sub> capacity level represents the quantity of hydrogen that could be used for each cycle (i.e. stored then unloaded) and is calculated by subtracting the DoH to the DoDH for each cycle *x*, using the equation (5)(ESI S5):

$$\begin{aligned} H_2 \text{ capacity level}_{\text{cycle } x} &= DoH_{\text{after the hydrogenation cycle } x} \\ &- DoH_{\text{after the dehydrogenation cycle } x} \end{aligned} \quad (5)$$

Upon multiple cycles, impurities form in the system, which change the maximum theoretical hydrogen storage capacity. Most of these impurities are already studied LOHC couples such as Ethylbenzene/Ethylcyclohexane. Hence, the degree of hydrogenation and dehydrogenation is modified in order to account for the cycling of the impurities. A partial degree of hydrogenation or dehydrogenation is calculated for each of the LOHC couples and is then calculated by multiplying each partial degree of hydrogenation or dehydrogenation with the molar fraction of these compounds in the reactional mixture at the start of the step, using the equation (6) An example of this calculation is given in the ESI (S4).

$$DoH_{\text{cycling}} = \sum_i (\text{mol}\%_i \times DoH \text{ or } DoDH_i) \quad (6)$$

#### Kinetics

10 mL of CHEA were dehydrogenated with 0.25 wt% of the optimized Pt/C catalyst at 205 °C in argon atmosphere. Aliquots equivalent to a drop of the reaction mixture were manually sampled at regular time intervals: every 5 min before 15 min, then every 15 min until 1 h, then every hour until 8 h and finally every 2 h each day until the end of the reaction. These aliquots were analysed by GC-MS, being beforehand diluted in the GC-MS solvent and filtered with a syringe filter (0.45 µm) to remove the catalyst.

#### Activation energy

The activation energy for each function of the LOHC system (cycloalkane/aromatic and alcohol/ketone) was measured during the dehydrogenation. Chemical kinetics were performed at different temperatures (190, 205 and 210 °C) over a week, so that the equilibrium state could be achieved for each function at the desired temperature. The reactions were performed under a 10 mL/min flux of 5% H<sub>2</sub> in Argon in order to remove the concentration of H<sub>2</sub> as a parameter in the kinetics laws. As the kinetics laws of the reaction are highly complex for sequential and branched reversible reactions, a lumped kinetics approach was proposed to simplify the reaction mechanism. This approach is pertinent for complex kinetics systems and yields kinetic parameters with good accuracy.[83] Aliquots of the reaction mixture were sampled at regular time intervals and were analysed by GC-MS, being beforehand diluted in the GC-MS solvent and filtered with a syringe filter (0.45 µm) to remove the catalyst.

#### DFT

All computations have been performed with the Gaussian 16 Rev C.01 suite, using the hybrid meta-GGA functional M06-2X and the basis set 6-311+G(2d,p) for elements. Such parameters are known to predict accurately the thermochemistry of main-group compounds in the ground-state as well as polyenes systems. Each structure is solvated in Acetophenone using the SMD model which is recommended to compute thermochemical parameters. Frequency calculations were performed on the optimized structures using the same parameters; all structures were verified to possess no imaginary frequencies.

#### Catalyst synthesis

A wet-impregnation method was used for the preparation of the 2wt% Pt/Al<sub>2</sub>O<sub>3</sub> catalysts. Typically, acidic Al<sub>2</sub>O<sub>3</sub> (2.0 g) was mixed with an aqueous solution of H<sub>2</sub>PtCl<sub>6</sub> (4.5 gPt/L), with the volume of the latter being tuned to the target loading of Pt, and the slurry was stirred at room temperature until the water was evaporated. The solid mixture was then dried at 100 °C in air overnight in an oven. The resulting solid was milled into a fine powder and then calcined in air (550 °C, heating rate: 3 °C/min). The calcined catalysts were reduced in a tubular oven under Ar/H<sub>2</sub> flow (2.5%; 100 mL/min) at a selected temperature (250 °C, heating rate 3 °C/min) for 2 h.

## Acknowledgments

We thank Christophe Brouard (CEA Grenoble) for the preparation and analysis of samples by ICP-OES. We thank Nathalie Pelissier (CEA Grenoble) for the preparation and analysis of samples by TEM-EDS. We thank Dr. Raphael Ramos (CEA Grenoble) for the preparation, analysis and interpretation of samples by Raman spectroscopy. We thank Dr. Anass Benayad (CEA Grenoble) for his help in the interpretation of samples by XPS.

This work was supported by the CEA, the CNRS, the University Paris-Saclay, CINES (HPC Computing time on Occigen, grant no. A010806494), the European Research Council (ERC Consolidator Grant Agreement no. 818260) and the European project funding from the Fuel Cells and Hydrogen 2 Joint Undertaking under grant agreement No 101007223. T.C. thanks the Fondation Louis D.–Institut de France for its major support.

## References

- [1] Gupta RB. Hydrogen Fuel: Production, Transport, and Storage. CRC Press; 2008.
- [2] Orecchini F. The era of energy vectors. *International Journal of Hydrogen Energy* 2006;31:1951–4. <https://doi.org/10.1016/j.ijhydene.2006.01.015>.
- [3] Kar SK, Harichandan S, Roy B. Bibliometric analysis of the research on hydrogen economy: An analysis of current findings and roadmap ahead. *International Journal of Hydrogen Energy* 2022. <https://doi.org/10.1016/j.ijhydene.2022.01.137>.
- [4] Reuß M, Grube T, Robinius M, Preuster P, Wasserscheid P, Stolten D. Seasonal storage and alternative carriers: A flexible hydrogen supply chain model. *Applied Energy* 2017;200:290–302. <https://doi.org/10.1016/j.apenergy.2017.05.050>.
- [5] Grünenfelder NF, Schucan ThH. Seasonal storage of hydrogen in liquid organic hydrides: description of the second prototype vehicle. *International Journal of Hydrogen Energy* 1989;14:579–86. [https://doi.org/10.1016/0360-3199\(89\)90117-1](https://doi.org/10.1016/0360-3199(89)90117-1).
- [6] Züttel A. Hydrogen storage methods. *Naturwissenschaften* 2004;91:157–72. <https://doi.org/10.1007/s00114-004-0516-x>.
- [7] He T, Pei Q, Chen P. Liquid organic hydrogen carriers. *Journal of Energy Chemistry* 2015;24:587–94. <https://doi.org/10.1016/j.jechem.2015.08.007>.
- [8] Cho J-Y, Kim H, Oh J-E, Park BY. Recent Advances in Homogeneous/Heterogeneous Catalytic Hydrogenation and Dehydrogenation for Potential Liquid Organic Hydrogen Carrier (LOHC) Systems. *Catalysts* 2021;11:1497. <https://doi.org/10.3390/catal11121497>.
- [9] Teichmann D, Arlt W, Wasserscheid P. Liquid Organic Hydrogen Carriers as an efficient vector for the transport and storage of renewable energy. *International Journal of Hydrogen Energy* 2012;37:18118–32. <https://doi.org/10.1016/j.ijhydene.2012.08.066>.
- [10] Taube M, Rippin D, Knecht W, Hakimifard D, Milisavljevic B, Gruenenfelder N. A prototype truck powered by hydrogen from organic liquid hydrides. *International Journal of Hydrogen Energy* 1985;10:595–9. [https://doi.org/10.1016/0360-3199\(85\)90035-7](https://doi.org/10.1016/0360-3199(85)90035-7).
- [11] Target Explanation Document: Onboard Hydrogen Storage for Light-Duty Fuel Cell Vehicles. EnergyGov n.d. <https://www.energy.gov/eere/fuelcells/downloads/target-explanation-document-onboard-hydrogen-storage-light-duty-fuel-cell> (accessed June 4, 2021).

- [12] Alan C. Cooper. Design and Development of New Carbon-Based Sorbent Systems for an Effective Containment of Hydrogen. 2012. <https://doi.org/10.2172/1039432>.
- [13] Clot E, Eisenstein O, H. Crabtree R. Computational structure–activity relationships in H<sub>2</sub> storage: how placement of N atoms affects release temperatures in organic liquid storage materials. *Chemical Communications* 2007;0:2231–3. <https://doi.org/10.1039/B705037B>.
- [14] Cui Y, Kwok S, Bucholtz A, Davis B, A. Whitney R, G. Jessop P. The effect of substitution on the utility of piperidines and octahydroindoles for reversible hydrogen storage. *New Journal of Chemistry* 2008;32:1027–37. <https://doi.org/10.1039/B718209K>.
- [15] Enthaler S, Langermann J von, Schmidt T. Carbon dioxide and formic acid—the couple for environmental-friendly hydrogen storage? *Energy Environ Sci* 2010;3:1207–17. <https://doi.org/10.1039/B907569K>.
- [16] Tseng K-NT, Rizzi AM, Szymczak NK. Oxidant-Free Conversion of Primary Amines to Nitriles. *J Am Chem Soc* 2013;135:16352–5. <https://doi.org/10.1021/ja409223a>.
- [17] Siddiki SMAH, Toyao T, Shimizu K. Acceptorless dehydrogenative coupling reactions with alcohols over heterogeneous catalysts. *Green Chemistry* 2018;20:2933–52. <https://doi.org/10.1039/C8GC00451J>.
- [18] Gould ES. Mechanism and structure in organic chemistry. Holt, Rinehart and Winston; 1959.
- [19] S. Luterbacher J, Alonso DM, A. Dumesic J. Targeted chemical upgrading of lignocellulosic biomass to platform molecules. *Green Chemistry* 2014;16:4816–38. <https://doi.org/10.1039/C4GC01160K>.
- [20] Mitsudome T, Mikami Y, Ebata K, Mizugaki T, Jitsukawa K, Kaneda K. Copper nanoparticles on hydrotalcite as a heterogeneous catalyst for oxidant-free dehydrogenation of alcohols. *Chemical Communications* 2008;0:4804–6. <https://doi.org/10.1039/B809012B>.
- [21] Zhang P, Wang Q-N, Yang X, Wang D, Li W-C, Zheng Y, et al. A Highly Porous Carbon Support Rich in Graphitic-N Stabilizes Copper Nanocatalysts for Efficient Ethanol Dehydrogenation. *ChemCatChem* 2017;9:505–10. <https://doi.org/10.1002/cctc.201601373>.
- [22] Miura H, Nakahara K, Kitajima T, Shishido T. Concerted Functions of Surface Acid–Base Pairs and Supported Copper Catalysts for Dehydrogenative Synthesis of Esters from Primary Alcohols. *ACS Omega* 2017;2:6167–73. <https://doi.org/10.1021/acsomega.7b01142>.
- [23] McCullough LR, Childers DJ, Watson RA, Kilos BA, Barton DG, Weitz E, et al. Acceptorless Dehydrogenative Coupling of Neat Alcohols Using Group VI Sulfide Catalysts. *ACS Sustainable Chem Eng* 2017;5:4890–6. <https://doi.org/10.1021/acssuschemeng.7b00303>.
- [24] Falbe J, Bahrmann H, Lipps W, Mayer D, Frey GD. Alcohols, Aliphatic. *Ullmann's Encyclopedia of Industrial Chemistry*, John Wiley & Sons, Ltd; 2013. [https://doi.org/10.1002/14356007.a01\\_279.pub2](https://doi.org/10.1002/14356007.a01_279.pub2).
- [25] Kohlpaintner C, Schulte M, Falbe J, Lappe P, Weber J, Frey GD. Aldehydes, Aliphatic. *Ullmann's Encyclopedia of Industrial Chemistry*, John Wiley & Sons, Ltd; 2013. [https://doi.org/10.1002/14356007.a01\\_321.pub3](https://doi.org/10.1002/14356007.a01_321.pub3).
- [26] Kohlpaintner C, Schulte M, Falbe J, Lappe P, Weber J, Frey GD. Aldehydes, Aliphatic. *Ullmann's Encyclopedia of Industrial Chemistry*, John Wiley & Sons, Ltd; 2013. [https://doi.org/10.1002/14356007.m01\\_m03.pub2](https://doi.org/10.1002/14356007.m01_m03.pub2).
- [27] Siegel H, Eggersdorfer M. Ketones. *Ullmann's Encyclopedia of Industrial Chemistry*, John Wiley & Sons, Ltd; 2000. [https://doi.org/10.1002/14356007.a15\\_077](https://doi.org/10.1002/14356007.a15_077).
- [28] Kaźmierczak K, Salisu A, Pinel C, Besson M, Michel C, Perret N. Activity of heterogeneous supported Cu and Ru catalysts in acceptor-less alcohol dehydrogenation. *Catalysis Communications* 2021;148:106179. <https://doi.org/10.1016/j.catcom.2020.106179>.
- [29] Guerrero-Ruiz A, Rodriguez-Ramos I, Fierro JLG. Dehydrogenation of methanol to methyl formate over supported copper catalysts. *Applied Catalysis* 1991;72:119–37. [https://doi.org/10.1016/0166-9834\(91\)85033-R](https://doi.org/10.1016/0166-9834(91)85033-R).
- [30] Ichikawa N, Sato S, Takahashi R, Sodesawa T, Inui K. Dehydrogenative cyclization of 1,4-butanediol over copper-based catalyst. *Journal of Molecular Catalysis A: Chemical* 2004;212:197–203. <https://doi.org/10.1016/j.molcata.2003.10.028>.

- [31] Vorotnikov V, Mpourmpakis G, Vlachos DG. DFT Study of Furfural Conversion to Furan, Furfuryl Alcohol, and 2-Methylfuran on Pd(111). *ACS Catal* 2012;2:2496–504. <https://doi.org/10.1021/cs300395a>.
- [32] Merat N, Godawa C, Gaset A. High selective production of tetrahydrofurfuryl alcohol: Catalytic hydrogenation of furfural and furfuryl alcohol. *Journal of Chemical Technology & Biotechnology* 1990;48:145–59. <https://doi.org/10.1002/jctb.280480205>.
- [33] Claus P, Berndt H, Mohr C, Radnik J, Shin E-J, Keane MA. Pd/MgO: Catalyst Characterization and Phenol Hydrogenation Activity. *Journal of Catalysis* 2000;192:88–97. <https://doi.org/10.1006/jcat.2000.2834>.
- [34] Zhang J, Jiang Q, Yang D, Zhao X, Dong Y, Liu R. Reaction-activated palladium catalyst for dehydrogenation of substituted cyclohexanones to phenols and H<sub>2</sub> without oxidants and hydrogen acceptors. *Chemical Science* 2015;6:4674–80. <https://doi.org/10.1039/C5SC01044F>.
- [35] Kleinert M, Barth T. Phenols from Lignin. *Chemical Engineering & Technology* 2008;31:736–45. <https://doi.org/10.1002/ceat.200800073>.
- [36] Weber M, Weber M, Kleine-Boymann M. Phenol. *Ullmann's Encyclopedia of Industrial Chemistry*, John Wiley & Sons, Ltd; 2004. [https://doi.org/10.1002/14356007.a19\\_299.pub2](https://doi.org/10.1002/14356007.a19_299.pub2).
- [37] Zakgeym D, David Hofmann J, Andreas Maurer L, Auer F, Müller K, Wolf M, et al. Better through oxygen functionality? The benzophenone/dicyclohexylmethanol LOHC-system. *Sustainable Energy & Fuels* 2023. <https://doi.org/10.1039/D2SE01750D>.
- [38] Brückner N, Obesser K, Bösmann A, Teichmann D, Arlt W, Dungs J, et al. Evaluation of Industrially Applied Heat-Transfer Fluids as Liquid Organic Hydrogen Carrier Systems. *ChemSusChem* 2014;7:229–35. <https://doi.org/10.1002/cssc.201300426>.
- [39] Luo N, Wang M, Li H, Zhang J, Hou T, Chen H, et al. Visible-Light-Driven Self-Hydrogen Transfer Hydrogenolysis of Lignin Models and Extracts into Phenolic Products. *ACS Catal* 2017;7:4571–80. <https://doi.org/10.1021/acscatal.7b01043>.
- [40] Theilacker W, Drössler H-G. Die katalytische Hydrierung von Acetophenon mit Platin und Palladium. Ein Beitrag zur Selektivität der Edelmetallkatalysatoren. *Chemische Berichte* 1954;87:1676–84. <https://doi.org/10.1002/cber.19540871111>.
- [41] Kim W-H, Park IS, Park J. Acceptor-Free Alcohol Dehydrogenation by Recyclable Ruthenium Catalyst. *Org Lett* 2006;8:2543–5. <https://doi.org/10.1021/ol060750z>.
- [42] Putro WS, Kojima T, Hara T, Ichikuni N, Shimazu S. Acceptorless dehydrogenation of alcohols using Cu–Fe catalysts prepared from Cu–Fe layered double hydroxides as precursors. *Catal Sci Technol* 2018;8:3010–4. <https://doi.org/10.1039/C8CY00655E>.
- [43] Burgener M, Mallat T, Baiker A. Palladium-catalysed dehydrogenation of 1-phenylethanol in dense carbon dioxide. *Journal of Molecular Catalysis A: Chemical* 2005;225:21–5. <https://doi.org/10.1016/j.molcata.2004.08.029>.
- [44] Tilgner D, Klarner M, Hammon S, Friedrich M, Verch A, Jonge N de, et al. H<sub>2</sub>-Generation from Alcohols by the MOF-Based Noble Metal-Free Photocatalyst Ni/CdS/TiO<sub>2</sub>@MIL-101\*. *Aust J Chem* 2019;72:842–7. <https://doi.org/10.1071/CH19255>.
- [45] Mitsudome T, Mikami Y, Funai H, Mizugaki T, Jitsukawa K, Kaneda K. Oxidant-Free Alcohol Dehydrogenation Using a Reusable Hydrotalcite-Supported Silver Nanoparticle Catalyst. *Angewandte Chemie International Edition* 2008;47:138–41. <https://doi.org/10.1002/anie.200703161>.
- [46] Fang W, Zhang Q, Chen J, Deng W, Wang Y. Gold nanoparticles on hydrotalcites as efficient catalysts for oxidant-free dehydrogenation of alcohols. *Chem Commun* 2010;46:1547–9. <https://doi.org/10.1039/B923047E>.
- [47] Fujita K, Tanino N, Yamaguchi R. Ligand-Promoted Dehydrogenation of Alcohols Catalyzed by Cp\*Ir Complexes. A New Catalytic System for Oxidant-Free Oxidation of Alcohols. *Org Lett* 2007;9:109–11. <https://doi.org/10.1021/ol062806v>.
- [48] Falini G, Gualandi A, Savoia D. Rhodium/Graphite-Catalyzed Hydrogenation of Carbocyclic and Heterocyclic Aromatic Compounds. *Synthesis* 2009;2009:2440–6. <https://doi.org/10.1055/s-0029-1216852>.

- [49] Llop Castelbou J, Bresó-Femenia E, Blondeau P, Chaudret B, Castellón S, Claver C, et al. Tuning the Selectivity in the Hydrogenation of Aromatic Ketones Catalyzed by Similar Ruthenium and Rhodium Nanoparticles. *ChemCatChem* 2014;6:3160–8. <https://doi.org/10.1002/cctc.201402524>.
- [50] Masson J, Cividino P, Court J. Selective hydrogenation of acetophenone on chromium promoted Raney nickel catalysts. III. The influence of the nature of the solvent. *Applied Catalysis A: General* 1997;161:191–7. [https://doi.org/10.1016/S0926-860X\(97\)00068-9](https://doi.org/10.1016/S0926-860X(97)00068-9).
- [51] JOBACK KG, REID RC. Estimation of Pure-Component Properties from Group-Contributions. *Chemical Engineering Communications* 1987;57:233–43. <https://doi.org/10.1080/00986448708960487>.
- [52] Rousset JL, Stievano L, Aires FJCS, Geantet C, Renouprez AJ, Pellarin M. Hydrogenation of Toluene over  $\gamma$ -Al<sub>2</sub>O<sub>3</sub>-Supported Pt, Pd, and Pd–Pt Model Catalysts Obtained by Laser Vaporization of Bulk Metals. *Journal of Catalysis* 2001;197:335–43. <https://doi.org/10.1006/jcat.2000.3083>.
- [53] Chen M, Maeda N, Baiker A, Huang J. Hydrogenation of Acetophenone on Pd/Silica–Alumina Catalysts with Tunable Acidity: Mechanistic Insight by In Situ ATR-IR Spectroscopy. *ACS Catal* 2018;8:6594–600. <https://doi.org/10.1021/acscatal.8b00169>.
- [54] Do G, Preuster P, Aslam R, Bösmann A, Müller K, Arlt W, et al. Hydrogenation of the liquid organic hydrogen carrier compound dibenzyltoluene – reaction pathway determination by <sup>1</sup>H NMR spectroscopy. *Reaction Chemistry & Engineering* 2016;1:313–20. <https://doi.org/10.1039/C5RE00080G>.
- [55] Jorschick H, Preuster P, Dürr S, Seidel A, Müller K, Bösmann A, et al. Hydrogen storage using a hot pressure swing reactor. *Energy & Environmental Science* 2017;10:1652–9. <https://doi.org/10.1039/C7EE00476A>.
- [56] Suppino RS, Landers R, Cobo AJG. Influence of noble metals (Pd, Pt) on the performance of Ru/Al<sub>2</sub>O<sub>3</sub> based catalysts for toluene hydrogenation in liquid phase. *Applied Catalysis A: General* 2016;525:41–9. <https://doi.org/10.1016/j.apcata.2016.06.038>.
- [57] Bianchi CL, Ragaini V, Cattania MG. An XPS study on ruthenium compounds and catalysts. *Materials Chemistry and Physics* 1991;29:297–306. [https://doi.org/10.1016/0254-0584\(91\)90025-P](https://doi.org/10.1016/0254-0584(91)90025-P).
- [58] Kim KS, Winograd N. X-Ray photoelectron spectroscopic studies of ruthenium-oxygen surfaces. *Journal of Catalysis* 1974;35:66–72. [https://doi.org/10.1016/0021-9517\(74\)90184-5](https://doi.org/10.1016/0021-9517(74)90184-5).
- [59] Chen S, Abdel-Mageed AM, Dyballa M, Parlinska-Wojtan M, Bansmann J, Pollastri S, et al. Raising the CO<sub>x</sub> Methanation Activity of a Ru/ $\gamma$ -Al<sub>2</sub>O<sub>3</sub> Catalyst by Activated Modification of Metal–Support Interactions. *Angewandte Chemie International Edition* 2020;59:22763–70. <https://doi.org/10.1002/anie.202007228>.
- [60] Durndell LJ, Zou G, Shangguan W, Lee AF, Wilson K. Structure-Reactivity Relations in Ruthenium Catalysed Furfural Hydrogenation. *ChemCatChem* 2019;11:3927–32. <https://doi.org/10.1002/cctc.201900481>.
- [61] Mazzieri V, Coloma-Pascual F, Arcoya A, L'Argentièrre PC, Fígoli NS. XPS, FTIR and TPR characterization of Ru/Al<sub>2</sub>O<sub>3</sub> catalysts. *Applied Surface Science* 2003;210:222–30. [https://doi.org/10.1016/S0169-4332\(03\)00146-6](https://doi.org/10.1016/S0169-4332(03)00146-6).
- [62] bvcrist. Aluminum Spectra - Al(OH)<sub>3</sub>. The International XPS Database 1 n.d. <https://xpsdatabase.com/aluminum-spectra-aloh3/> (accessed October 14, 2022).
- [63] bvcrist. Aluminum Spectra -  $\alpha$ -Al<sub>2</sub>O<sub>3</sub>. The International XPS Database 1 n.d. <https://xpsdatabase.com/aluminum-spectra-al2o3/> (accessed October 14, 2022).
- [64] Karvembu R, Prabhakaran R, Senthilkumar K, Viswanathamurthi P, Natarajan K. Ru/Al<sub>2</sub>O<sub>3</sub>-catalyzed transfer dehydrogenation of alcohols. *React Kinet Catal Lett* 2005;86:211–6. <https://doi.org/10.1007/s11144-005-0314-2>.
- [65] Yergaziyeva GY, Dossumov K, Mambetova MM, Strizhak PY, Kurokawa H, Baizhomartov B. Effect of Ni, La, and Ce Oxides on a Cu/Al<sub>2</sub>O<sub>3</sub> Catalyst with Low Copper Loading for Ethanol Non-



- oxidative Dehydrogenation. *Chemical Engineering & Technology* 2021;44:1890–9. <https://doi.org/10.1002/ceat.202100112>.
- [66] Xia Z, Lu H, Liu H, Zhang Z, Chen Y. Cyclohexane dehydrogenation over Ni-Cu/SiO<sub>2</sub> catalyst: Effect of copper addition. *Catalysis Communications* 2017;90:39–42. <https://doi.org/10.1016/j.catcom.2016.10.036>.
- [67] Nicolau G, Tarantino G, Hammond C. Acceptorless Alcohol Dehydrogenation Catalysed by Pd/C. *ChemSusChem* 2019;12:4953–61. <https://doi.org/10.1002/cssc.201901313>.
- [68] Wang J, Liu H, Fan S, Wang S, Xu G, Guo A, et al. Dehydrogenation of Cycloalkanes over N-Doped Carbon-Supported Catalysts: The Effects of Active Component and Molecular Structure of the Substrate. *Nanomaterials* 2021;11:2846. <https://doi.org/10.3390/nano11112846>.
- [69] Modisha P, Gqogqa P, Garidzirai R, Ouma CNM, Bessarabov D. Evaluation of catalyst activity for release of hydrogen from liquid organic hydrogen carriers. *International Journal of Hydrogen Energy* 2019;44:21926–35. <https://doi.org/10.1016/j.ijhydene.2019.06.212>.
- [70] Yang M, Dong Y, Fei S, Ke H, Cheng H. A comparative study of catalytic dehydrogenation of perhydro-N-ethylcarbazole over noble metal catalysts. *International Journal of Hydrogen Energy* 2014;39:18976–83. <https://doi.org/10.1016/j.ijhydene.2014.09.123>.
- [71] Kim H-J, Kim W-I, Park T-J, Park H-S, Suh DJ. Highly dispersed platinum–carbon aerogel catalyst for polymer electrolyte membrane fuel cells. *Carbon* 2008;46:1393–400. <https://doi.org/10.1016/j.carbon.2008.05.022>.
- [72] Wang L, Roudgar A, Eikerling M. Ab Initio Study of Stability and Site-Specific Oxygen Adsorption Energies of Pt Nanoparticles. *J Phys Chem C* 2009;113:17989–96. <https://doi.org/10.1021/jp900965q>.
- [73] Helfferich FG, Compton RG, Bamford CH. *Comprehensive chemical kinetics*. Elsevier; 2001.
- [74] Rioux RM, Vannice MA. Dehydrogenation of isopropyl alcohol on carbon-supported Pt and Cu–Pt catalysts. *Journal of Catalysis* 2005;233:147–65. <https://doi.org/10.1016/j.jcat.2005.04.020>.
- [75] A. Jones RW, R. Thomas JD. Steric influence of the alkyl component in the alkaline hydrolysis of acetates and propionates. *Journal of the Chemical Society B: Physical Organic* 1966;0:661–4. <https://doi.org/10.1039/J29660000661>.
- [76] Galimova NA, Pskhu ZV, Naumkin AV, Volkov IO, Yagodovskaya TV, Yagodovskii VD. The influence of plasma chemical treatment of a platinum catalyst on its activity in the dehydrogenation of cyclohexane. *Russ J Phys Chem* 2009;83:1720–6. <https://doi.org/10.1134/S0036024409100161>.
- [77] Shuikin NI, Levitsky II. High temperature catalytic dehydrogenation of ethylcyclohexane. *Russ Chem Bull* 1953;2:895–902. <https://doi.org/10.1007/BF01167533>.
- [78] Lee J-Y, Yung T-Y, Liu L-K. The microwave-assisted ionic liquid nanocomposite synthesis: platinum nanoparticles on graphene and the application on hydrogenation of styrene. *Nanoscale Research Letters* 2013;8:414. <https://doi.org/10.1186/1556-276X-8-414>.
- [79] Knözinger H. Dehydration of Alcohols on Aluminum Oxide. *Angewandte Chemie International Edition in English* 1968;7:791–805. <https://doi.org/10.1002/anie.196807911>.
- [80] Zuffanti S, Luder WF. Generalized acids and bases in organic chemistry. I. Catalytic condensation of aldehydes. *J Chem Educ* 1944;21:485. <https://doi.org/10.1021/ed021p485>.
- [81] Guthrie JP, Cossar J, Cullimore PA, Kamkar NM, Taylor KF. The retroaldol reaction of chalcone. *Can J Chem* 1983;61:2621–6. <https://doi.org/10.1139/v83-449>.
- [82] Kurti L, Czako B. *Strategic Applications of Named Reactions in Organic Synthesis*. Elsevier; 2005.
- [83] Pico MP, Romero A, Rodríguez S, Santos A. Etherification of Glycerol by tert-Butyl Alcohol: Kinetic Model. *Ind Eng Chem Res* 2012;51:9500–9. <https://doi.org/10.1021/ie300481d>.